

# 3D segmentation of mandible from multisectional CT scans by convolutional neural networks

Bingjiang Qiu<sup>1,2</sup>, Jiapan Guo<sup>4,6</sup>, J. Kraeima<sup>1,3</sup>, R.J.H. Borra<sup>2,5</sup>,  
M.J.H. Witjes<sup>1,3</sup> and P.M.A. van Ooijen<sup>1,2</sup>

<sup>1</sup>3D Lab, <sup>2</sup> Department of Radiology, <sup>3</sup>Department of Oral and Maxillofacial Surgery,  
<sup>4</sup>Center for Medical Imaging, <sup>5</sup>Department of Nuclear Medicine and Molecular  
Imaging, <sup>6</sup>Corresponding author  
University Medical Centre Groningen, Hanzeplein 1, 9713GZ, Groningen, The  
Netherlands

E-mail: j.guo@umcg.nl

September 2018

**Abstract.** Segmentation of mandibles in CT scans during virtual surgical planning is crucial for 3D surgical planning in order to obtain a detailed surface representation of the patients bone. Automatic segmentation of mandibles in CT scans is a challenging task due to large variation in their shape and size between individuals. In order to address this challenge we propose a convolutional neural network approach for mandible segmentation in CT scans by considering the continuum of anatomical structures through different planes. The proposed convolutional neural network adopts the architecture of the U-Net and then combines the resulting 2D segmentations from three different planes into a 3D segmentation. We implement such a segmentation approach on 11 neck CT scans and then evaluate the performance. We achieve an average dice coefficient of 0.89 on two testing mandible segmentation. Experimental results show that our proposed approach for mandible segmentation in CT scans exhibits high accuracy.

## 1. Introduction

### 1.1. Motivation

Three-dimensional virtual surgical planning (3D VSP) provides a precise and predictable method for bone related craniofacial tumor resection and free flap reconstruction of the reseted mandible. It is performed pre-operatively to determine the resection margins and cutting planes. The planning is translated towards the actual surgical procedure by the use of patient specific 3D printed guides. Computed tomography (CT) is the most commonly used modality for implementing such a process. Manual segmentation of the mandible in CT, however, leads to a tedious procedure in the clinical practice. Moreover, the structural complexity of mandibles and the considerable inter- and intra-rater variability make the segmentation of mandibles in CT scans challenging.

## *1.2. Related works*

In the past decades, several semi-automatic and automatic methods have been developed to segment the mandible in CT scans. In multiple publications conventional methods have been proposed (Gollmer & Buzug 2012)(Torosdagli, Liberton, Verma, Sincan, Lee, Pattanaik & Bagci 2017)(Chuang, Doherty, Adluru, Chung & Vorperian 2017)(Abdi, Kasaei & Mehdizadeh 2015). A statistical shape model for segmentation of the mandible was presented by Gollmer et al. (Gollmer & Buzug 2012) in 2012. Torosdagli et al. (Torosdagli et al. 2017) proposed an image segmentation algorithm using 3D gradient-based fuzzy connectedness to segment mandibles. A registration-based semiautomatic mandible segmentation technique was proposed by Chuang et al. (Chuang et al. 2017) in 2017. The studies of Abdi et al. (Abdi et al. 2015) show an automatic segmentation of mandible via collecting superior, inferior and exterior border in panoramic x-rays.

Since 2013, convolutional neural networks (CNNs) have been successfully applied in computer vision tasks, for examples, image classification, super-resolution, and semantic segmentation. Medical image segmentation, as one of the research focuses in semantic segmentation, has developed exponentially due to the rapid evolution of CNNs. Recent advances in semantic segmentation (Long, Shelhamer & Darrell 2015)(Badrinarayanan, Kendall & Cipolla 2017)(Ronneberger, Fischer & Brox 2015)(Yu & Koltun 2015)(Chen, Papandreou, Kokkinos, Murphy & Yuille 2018)(Lin, Milan, Shen & Reid 2017)(Zhao, Shi, Qi, Wang & Jia 2017)(Peng, Zhang, Yu, Luo & Sun 2017)(Chen, Papandreou, Schroff & Adam 2017)(Garcia-Garcia, Orts-Escolano, Oprea, Villena-Martinez & Garcia-Rodriguez 2017) have enabled their applications to medical image segmentation. Fully convolutional network (FCN) is one of the first methods that introduced CNN into semantic segmentation and showed its ability on training an end-to-end approach for image segmentation with arbitrary input image sizes (Long et al. 2015)(Garcia-Garcia et al. 2017). SegNet (Badrinarayanan et al. 2017) and U-Net (Ronneberger et al. 2015) are modified architectures based on FCN, that include an encoder and a decoder network. Both 3D-Unet (Çiçek, Abdulkadir, Lienkamp, Brox & Ronneberger 2016) and V-net (Milletari, Navab & Ahmadi 2016) are creative expansion techniques by taking into account the spatial information of medical images. The work in (Yu & Koltun 2015) proposed a multi-scale context aggregation module by dilated convolutions, which provides a solution to dense prediction problems in semantic segmentation. The use of dilated convolutions enables the enlargement of receptive fields without the increment of parameters and the loss of resolution. Deeplab (Chen et al. 2018) is an improved CNN architecture on semantic segmentation that uses dilated convolutions as well as conditional random fields. Refinenet (Lin et al. 2017) has a different architecture from that of the encoder-decoder mode. It makes use of all the information available along the down-sampling process to enable high-resolution prediction using long-range residual connections. The decoder part in Refinenet directly takes the feature maps of the encoder parts for fusion. PSPNet (Zhao et al. 2017) proposed a method of combining local and global information for dense prediction. An encoder-decoder structure with

a large-scale convolution kernel was proposed by Peng (Peng et al. 2017). Most of the above mentioned CNN architectures have been proven to be effective on semantic segmentation of natural scene images. Such works (Long et al. 2015)(Badrinarayanan et al. 2017)(Ronneberger et al. 2015)(Yu & Koltun 2015)(Chen et al. 2018)(Lin et al. 2017)(Zhao et al. 2017)(Peng et al. 2017)(Chen et al. 2017)(Garcia-Garcia et al. 2017) motivate our implementation of CNNs for automatic mandible segmentation in CT scans.

Considering the applications of these CNN approaches in medical image segmentation for anatomical structures, we could feed the medical imaging data into the CNN architectures in two ways: direct 3D data and 2D slice-by-slice data. Medical imaging datasets usually have a large number of images at high resolution. On the one hand, during a 3D segmentation, small volumetric patches are produced to feed into the CNNs in order to deal with memory issues. In such a way, it, however, loses the anatomical structural information comparing to the full volumetric data. On the other hand, 2D slice-by-slice segmentation cannot take into consideration the spatial information in depth. Thus, we propose a CNN based approach to deal with such situations in medical image segmentations, particularly in the segmentation of mandible from CT neck scans.

### *1.3. Contribution*

In this work, we propose a CNN-based approach for the automatic 3D segmentation of mandibles in CT neck scans. Such an approach uses multisectional CT data from different orthogonal planes as input and then combines the 2D segmentation results from each plane in order to achieve a mandible segmentation in a three dimensional view. Such a design of the system enables the consideration of similarity and structural continuity of the mandible from different planes. Experimental results on 11 CT data demonstrate the effectiveness of the proposed approach.

To summarize, the main contributions of this work are as follows:

- (i) To the best of our knowledge, this is the first work that uses deep learning approach to effectively segment the mandible in CT scans.
- (ii) The proposed approach extracts discriminate features from three orthogonal planes (axial, coronal and sagittal) which take into account the structural continuity of mandibles from different views.
- (iii) The achieved experimental results demonstrate that the feasibility and effectiveness of the proposed approach in 3D mandible segmentation.

## **2. Methods**

### *2.1. Network architecture*

In this work, we present a novel framework for the 3D segmentation of the mandible in CT scans. Figure 1 shows the architecture of the presented framework. Such a

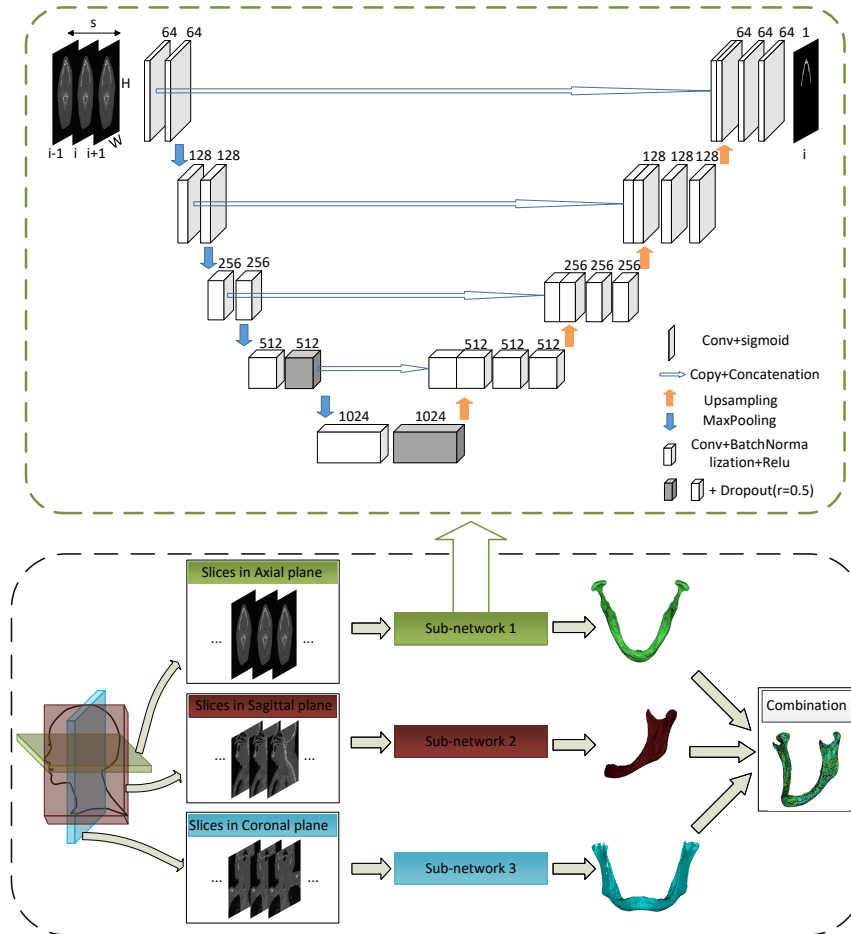


**Figure 1.** End-to-end architecture of the proposed convolutional neural network for 3D segmentation of the mandible, where  $H$ ,  $W$  and  $s$  represent the height, width and number of slices in the input layer, respectively. All the convolutional kernels have a size of  $3 \times 3$ .

framework consists of three parallel channels which segment the mandible from different orthogonal directions. Each of the channels has the same architecture of the U-Net. The 2D segmentation results from each channel are then combined into a 3D segmentation. In the following, we elaborate on how we built such a framework.

## 2.2. Single-channel CNN model

In this section, we elaborate on the design of the single channel module. Figure 1 (top row) shows the architecture of the single-channel module, which is inspired by the architecture of the U-Net (Ronneberger et al. 2015). In order to consider the similarity and continuity of upper and lower slice images of mandible, we apply multi-sectional images for training, which can maximally retain the structural information of

the mandible. This single-channel network consists of encoding and decoding procedures of in total 23 convolutional layers, in which size of each convolutional kernel is  $3 \times 3$ . The number of feature maps are listed on the top of each block that represents the convolutional layer. During the encoder procedure, max pooling layers are used to further enlarge the receptive fields. In order to achieve a pixel-wised classification, during the decoder procedure, upsampling layers are used and the feature maps are then concatenated with those of the same resolution from the decoder procedure. Different from that of the U-Net which concatenate the second feature maps from the same resolution in the encoder with those in the decoder, we pass the first block of feature maps to the decoder. Such a consideration helps to save computation resources.

Each of the convolutional layers is composed of a linear convolution, a batch normalization (Ioffe & Szegedy 2015) and an element-wise nonlinear Relu function (Nair & Hinton 2010). Finally the resulting responses are turned into probability values using a sigmoid classifier (Lin & Lin 2003). The output has the same size as that of the input image in the middle slice, as shown in Figure 1. In general, the convolutional layers (illustrated by the cubic blocks in Figure 1) can be expressed in the following equation:

$$L_i = \Gamma(L_{i-1} \otimes K_{ij} + B_i), \quad (1)$$

where  $L_i$  is an output of the  $i$ -th layer and the number of feature maps for  $L_i$  is shown in the top of each layer in Figure 1,  $\Gamma$  represents a nonlinear operator of Relu function,  $\otimes$  is a convolutional operator,  $K_{ij}$  means the  $j$ -st feature kernel in the  $i$ -st layer, and  $B_i$  denotes a bias of the  $i$ -st layer.

We use a loss function based on Dice coefficient which is commonly used to evaluate the performance of image segmentation tasks (Ghafoorian, Karssemeijer, Heskes, Uden, Sanchez, Litjens, Leeuw, Ginneken, Marchiori & Platel 2017). Detailed information about Dice can be found in Section 2.4.

### 2.3. Combination of the multi-sectional 2D mandible segmentation

The use of consecutive slices of scans helps improve the 2D segmentation of the mandible. However, on its own it does not provide satisfactory results since some parts of the mandible shapes are better observed via a different plane. Thus, we create a three channel network, of which each channel is fed with the CT data from a different orthogonal direction (axial, sagittal, coronal). We train these three channels separately using the corresponding data.

### 2.4. Loss metric

The Dice similarity index, also called the Dice score, is often used to measure consistency between two samples (Ghafoorian et al. 2017). Therefore, it is widely applied as a metric to evaluate the performance of image segmentation algorithms. It is defined as:

$$\text{Dice} = \frac{2|Y_r \cap Y_p|}{|Y_r| + |Y_p|}, \quad (2)$$

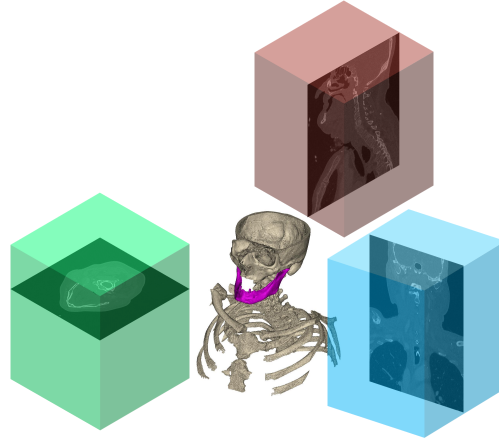


**Figure 2.** Example of a volumetric CT neck data. Such a scan contains 797 slices of CT images from the upper chest to the skull of a patient.

where  $Y_r$  is the reference standard, and  $Y_p$  is the predicted label from the network. Such a score has a value between 0 and 1, in which 0 means complete disagreement between the reference standard and the evaluated segmentation and 1 presents complete agreement. A differentiable technique has been used by Milletari (Milletari et al. 2016), which we utilize for minimizing the loss ( $\text{loss} = 1 - \text{Dice}$ ) between the two binary labels in training the presented model.

### 3. Experiments

#### 3.1. Data preparation

In our experiments, we use 11 CT scans reconstructed with a reconstruction kernel of Br64 or I70h(s). Each scan consists of 500 to 797 slices with  $512 \times 512$  pixels. We randomly choose eight cases as training, two cases as validation and one case as test. For ground truth, manual mandible segmentation was performed for each dataset using Materialise Mimics software<sup>‡</sup> by one trained researcher and confirmed by a clinician. Figure 2 shows an example of the data we use for our experiments.

#### 3.2. Training and test

The Keras (Chollet et al. 2015) package with the Tensorflow (Abadi, Agarwal, Barham, Brevdo, Chen, Citro, Corrado, Davis, Dean, Devin et al. 2016) backend is used to train our model on a workstation equipped with Nvidia Tesla K40m GPU of 12GB memory. After training the whole network for mandible segmentation, we apply the trained model

<sup>‡</sup> Mimics version 20.0 (Materialise, Leuven, Belgium)

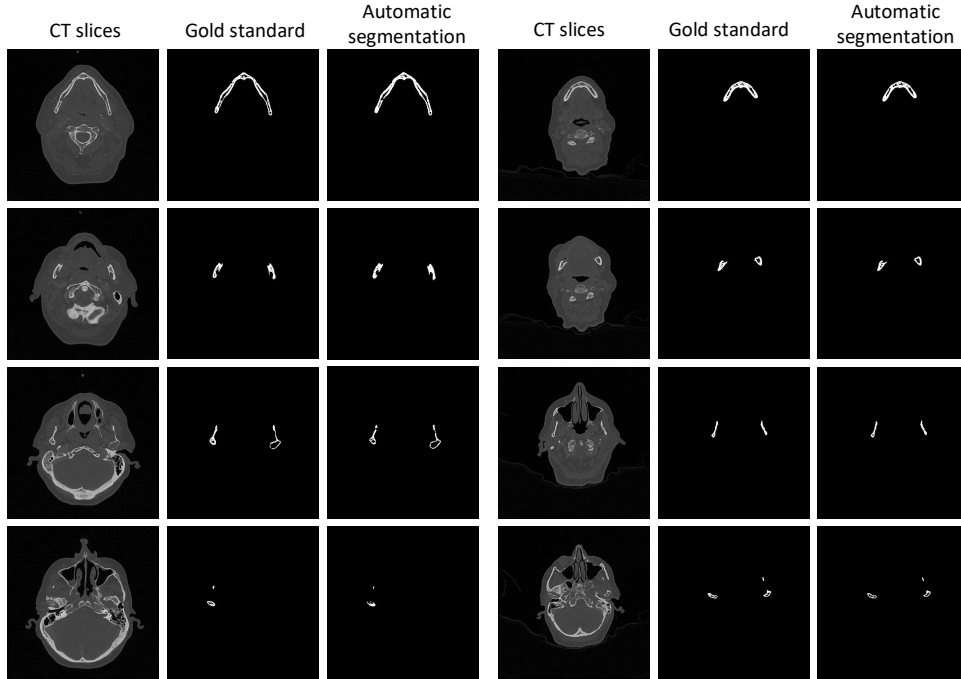


**Figure 3.** Examples of the automatic segmentation of mandibles in the axial plane.

to the test data. The time we used for training one single-channel model 30 epochs is 70 hours in total and the duration for testing the trained model on two various test datasets is 10 minutes. In the channel network fed with data from the axial plane, we set the input size of the data into  $H = 512$ ,  $W = 512$  and  $s = 3$ . In the Sagittal (Coronal) planes which often have different numbers of slices in every patients, we crop the input images into the same size of  $H = 400$ ,  $W = 400$  and  $s = 7$  ( $H = 400$ ,  $W = 400$  and  $s = 9$ ). We also use Adam optimization (Kingma & Ba 2014) with a learning rate of  $1 \times 10^{-5}$ . The three networks use the same size convolutions with zero padding. The entire architecture and parameters settings of the proposed model are shown in Figure 1.

### 3.3. Experimental results

We repeat the above mentioned process two times and then evaluate the performance of the proposed approach for automatic mandible segmentation. Figure 3 illustrates some examples of the results achieved by the proposed approach on the test data. The average Dice score of two case is 0.89. The distribution of the Dice score of every slice in two testing examples is illustrated in Figure 4. In Figure 4, we see that the segmentation accuracy in each image is about 0.9 comparing to the manual segmentation. This result indicates that the presented method is effective for 3D segmentation of mandible. To observe the experimental results visually, we used Materialise Mimics software to stack the 2D segmentation results into a 3D view, as shown in Figure 5.

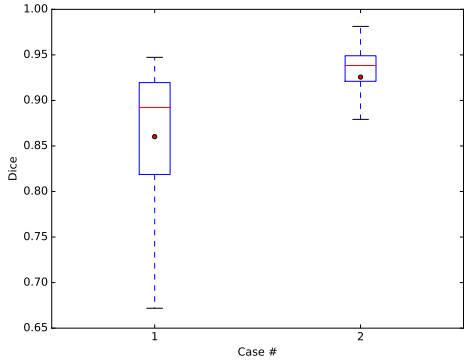


**Figure 4.** Box-whisker plot of the distribution of the dice coefficient from the test data. The red lines in the middle of the box indicates the median value of the dice while the red points represent the average dice coefficient.

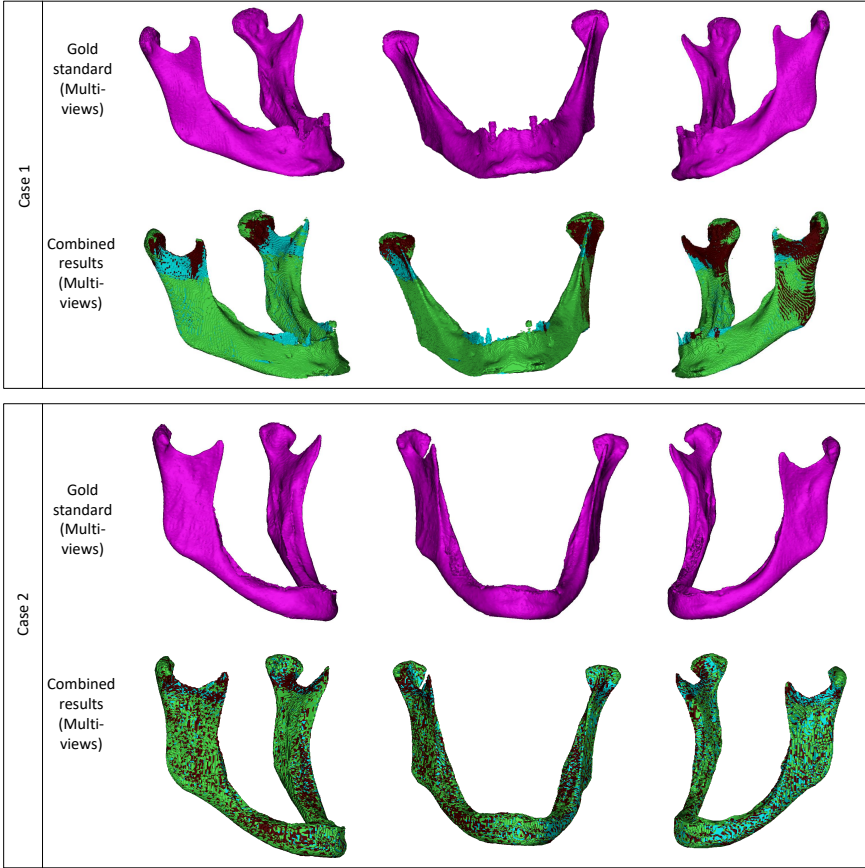


**Figure 5.** Resulting 3D model of two examples. Every column represents the 3D stacking models in left, middle and right angle of view, respectively. The 3D models in the first(third) row show the golden standard 3D model of the first(second) test case in the different views. The 3D models in the second(fourth) row show the resulting 3D model of the first(second) test case in the different views, in which green, brown and Royal blue mean subnet 1, subnet 2 and subnet 3, respectively.



#### **4. Discussion**

In this work, we present a CNN-based method for mandible segmentation. To the best of our knowledge, this is the first work to demonstrate that mandible in CT images can be effectively segmented using deep learning. In this work, we make full use of the extracted information from different directions to segment the mandible. Our proposed work indicates that 3-dimensional segmentation of medical images can also be achieved by 2D segmentation network which could help avoid the memory issues. Remarkably, this method has a good effect on mandible segmentation, even though until now only a small number of datasets was used during the training. Moreover, instead of using cropped images in some other works for 3D medical image segmentation [15][16], our approach uses the original size of all images, which maximally fits to the computation capacity of GPU and keeps the structural context of mandibles.

In the future, we could extend this work from the following directions. To begin with, the current implementation treats the corresponding 3D CT images segmentation of a mandible as a video object segmentation with continuous structure, in which we consider the special continuous structure of the mandible. Therefore, the technique of taking into account the neighbouring slices/frames information of each image could be adopted in the application of object segmentation in video frames. Moreover, the collection of contextual and shape information from different planes assures the sufficient extraction of useful information from input images, which could provide a future research direction for 3D image segmentation. Finally, the proposed work could be applied to other organ segmentation or in other imaging modalities, for example, MRI bone segmentation.

Further evaluation of our approach is required to assess its performance in clinical practice. This could be done through more massive and intensive experiments in or outside our maxillofacial oncology center. Additionally, only 11 patients data are annotated at this moment since the project is still in progress. More experimental datasets would be conducted to verify this technique in the near future. Besides, it is of great importance to verify the automatic mandible segmentation in the 3D virtual planning of craniofacial tumor resection and free flap reconstruction.

#### **5. Conclusion**

This paper proposed an end-to-end approach for automatic segmentation of mandible in CT scans. Such an approach has three channels for 2D segmentation of mandibles in multisectional CT scans and then combines the resulting 2D segmentation into 3D segmentation. We implement the proposed approach on 11 neck CT scans and achieve an average dice coefficient of 0.89. The experimental results demonstrate the effectiveness of the proposed approach in mandible segmentation and its potential employment in 3D virtual planning of craniofacial tumor resection and free flap reconstruction.

## References

- Abadi, M., Agarwal, A., Barham, P., Brevdo, E., Chen, Z., Citro, C., Corrado, G. S., Davis, A., Dean, J., Devin, M. et al. (2016). Tensorflow: Large-scale machine learning on heterogeneous distributed systems, *arXiv preprint arXiv:1603.04467*.
- Abdi, A. H., Kasaei, S. & Mehdizadeh, M. (2015). Automatic segmentation of mandible in panoramic x-ray, *Journal of Medical Imaging* **2**(4): 044003.
- Badrinarayanan, V., Kendall, A. & Cipolla, R. (2017). Segnet: A deep convolutional encoder-decoder architecture for image segmentation, *IEEE transactions on pattern analysis and machine intelligence* **39**(12): 2481–2495.
- Chen, L.-C., Papandreou, G., Kokkinos, I., Murphy, K. & Yuille, A. L. (2018). Deeplab: Semantic image segmentation with deep convolutional nets, atrous convolution, and fully connected crfs, *IEEE transactions on pattern analysis and machine intelligence* **40**(4): 834–848.
- Chen, L.-C., Papandreou, G., Schroff, F. & Adam, H. (2017). Rethinking atrous convolution for semantic image segmentation, *arXiv preprint arXiv:1706.05587*.
- Chollet, F. et al. (2015). Keras, <https://keras.io>.
- Chuang, Y. J., Doherty, B. M., Adluru, N., Chung, M. K. & Vorperian, H. K. (2017). A novel registration-based semiautomatic mandible segmentation pipeline using computed tomography images to study mandibular development, *Journal of computer assisted tomography*.
- Çiçek, Ö., Abdulkadir, A., Lienkamp, S. S., Brox, T. & Ronneberger, O. (2016). 3d u-net: learning dense volumetric segmentation from sparse annotation, *International Conference on Medical Image Computing and Computer-Assisted Intervention*, Springer, pp. 424–432.
- Garcia-Garcia, A., Orts-Escolano, S., Oprea, S., Villena-Martinez, V. & Garcia-Rodriguez, J. (2017). A review on deep learning techniques applied to semantic segmentation, *arXiv preprint arXiv:1704.06857*.
- Ghafoorian, M., Karssemeijer, N., Heskes, T., Uden, I. W., Sanchez, C. I., Litjens, G., Leeuw, F.-E., Ginneken, B., Marchiori, E. & Platel, B. (2017). Location sensitive deep convolutional neural networks for segmentation of white matter hyperintensities, *Scientific Reports* **7**(1): 5110.
- Gollmer, S. T. & Buzug, T. M. (2012). Fully automatic shape constrained mandible segmentation from cone-beam ct data, *Biomedical Imaging (ISBI), 2012 9th IEEE International Symposium on*, IEEE, pp. 1272–1275.
- Ioffe, S. & Szegedy, C. (2015). Batch normalization: Accelerating deep network training by reducing internal covariate shift, *arXiv preprint arXiv:1502.03167*.
- Kingma, D. P. & Ba, J. (2014). Adam: A method for stochastic optimization, *arXiv preprint arXiv:1412.6980*.
- Lin, G., Milan, A., Shen, C. & Reid, I. (2017). Refinenet: Multi-path refinement networks for high-resolution semantic segmentation, *IEEE Conference on Computer Vision and Pattern Recognition (CVPR)*.
- Lin, H.-T. & Lin, C.-J. (2003). A study on sigmoid kernels for svm and the training of non-psd kernels by smo-type methods, *submitted to Neural Computation* **3**: 1–32.
- Long, J., Shelhamer, E. & Darrell, T. (2015). Fully convolutional networks for semantic segmentation, *Proceedings of the IEEE conference on computer vision and pattern recognition*, pp. 3431–3440.
- Milletari, F., Navab, N. & Ahmadi, S.-A. (2016). V-net: Fully convolutional neural networks for volumetric medical image segmentation, *3D Vision (3DV), 2016 Fourth International Conference on*, IEEE, pp. 565–571.
- Nair, V. & Hinton, G. E. (2010). Rectified linear units improve restricted boltzmann machines, *Proceedings of the 27th international conference on machine learning (ICML-10)*, pp. 807–814.
- Peng, C., Zhang, X., Yu, G., Luo, G. & Sun, J. (2017). Large kernel matters—improve semantic segmentation by global convolutional network, *arXiv preprint arXiv:1703.02719*.
- Ronneberger, O., Fischer, P. & Brox, T. (2015). U-net: Convolutional networks for biomedical image segmentation, *International Conference on Medical image computing and computer-assisted*

*intervention*, Springer, pp. 234–241.

- Torosdagli, N., Liberton, D. K., Verma, P., Sincan, M., Lee, J., Pattanaik, S. & Bagci, U. (2017). Robust and fully automated segmentation of mandible from ct scans, *Biomedical Imaging (ISBI 2017), 2017 IEEE 14th International Symposium on*, IEEE, pp. 1209–1212.
- Yu, F. & Koltun, V. (2015). Multi-scale context aggregation by dilated convolutions, *arXiv preprint arXiv:1511.07122* .
- Zhao, H., Shi, J., Qi, X., Wang, X. & Jia, J. (2017). Pyramid scene parsing network, *IEEE Conf. on Computer Vision and Pattern Recognition (CVPR)*, pp. 2881–2890.